Mapping of $Al_xGa_{1-x}As$ band edges by ballistic electron emission spectroscopy

X.-C. Cheng,[a] D. A. Collins,[b] and T. C. McGill
Department of Applied Physics, California Institute of Technology, Pasadena, California 91125

(Received 11 October 1996; accepted 17 January 1997)

We have employed ballistic electron emission microscopy (BEEM) to study the energy positions in the conduction band of $Al_xGa_{1-x}As$. Epilayers of undoped $Al_xGa_{1-x}As$ were grown by molecular beam epitaxy on conductive GaAs substrates. The Al composition x took on values of 0, 0.11, 0.19, 0.25, 0.50, 0.80 and 1 so that the material was examined in both the direct and indirect band gap regime. The $Al_xGa_{1-x}As$ layer thickness was varied from 100 to 500 Å to ensure probing of bulk energy levels. Different capping layers and surface treatments were explored to prevent surface oxidation and examine Fermi level pinning at the cap layer/$Al_xGa_{1-x}As$ interface. All samples were metallized *ex situ* with a 100 Å Au layer so that the final BEEM structure is of the form Au/capping layer/$Al_xGa_{1-x}As$/bulk GaAs. Notably we have measured the Schottky barrier height for Au on $Al_xGa_{1-x}As$. We have also probed the higher lying band edges such as the X point at low Al concentrations and the L point at high Al concentrations. Variations of these critical energy positions with Al composition x were mapped out in detail and compared with findings from other studies. Local variations of these energy positions were also examined and found to be on the order of 30–50 meV. The results of this study suggest that BEEM can provide accurate positions for multiple energy levels in a single semiconductor structure. © *1997 American Vacuum Society.*
[S0734-2101(97)01104-4]

I. INTRODUCTION

Because of the technological importance of $Al_xGa_{1-x}As$, its various properties have been extensively studied. In particular, parameters of the $Al_xGa_{1-x}As$ band structure have been determined from a variety of measurements, including photoresponse,[1] optical transmission and photoluminescence,[2] variation of Hall electron concentration with temperature,[3] and variation of electrical conductivity with temperature.[4] However, there is some uncertainty about the exact positions of Γ, L, and X band edges, especially in the indirect band gap regime. Differences as much as 150 meV have been cited.[4] There is also a lack of consensus about the Au/$Al_xGa_{1-x}As$ Schottky barrier height at different Al concentrations,[17,18] which can be partly attributed to the various sample preparation procedures available.

This article describes the characterization of the above mentioned properties by ballistic electron emission microscopy (BEEM).[5,6] BEEM is a technique based on scanning tunnelling microscopy (STM). BEEM samples typically consist of a thin metal layer on top of a semiconductor of interest. The metal layer supports STM tunnel current while a new collector terminal at the back of the sample conducts away electrons that leak across the metal semiconductor interface. In BEEM spectroscopy, the collector current is monitored as a function of tunnelling voltage while the tunnelling current is kept constant by varying the STM tip to sample distance. As the tunnelling voltage increases and the STM tip potential rises above the bottom of the semiconductor conduction band, electrons can travel ballistically across the thin metal region and enter the semiconductor unimpeded, causing a noticeable increase in collector current. Bell and Kaiser developed a theory for the resulting collector current versus tunnelling voltage behavior by assuming transverse momentum conservation and no scattering at the metal semiconductor interface.[6] According to this model, BEEM collector current increases parabolically with tunnelling voltage near threshold. In cases where the semiconductor has higher lying conduction band edges, the BEEM I-V behavior may be modelled with several parabolic turn on's, each attributed to a band edge. Thus, by carefully analyzing BEEM I-V curves near threshold, one can delineate not only the metal Schottky barrier height but also higher lying band edges in the semiconductor provided that these energy positions are not too far apart. The scanning probe nature of BEEM allows the procedure to be carried out over different areas on the sample so that local variations these energy positions can be mapped out.

Since its inception, BEEM has been used extensively to study metal on semiconductor structures. It has been adapted by several workers to study the Schottky barrier height, higher lying band edge,[6] band offset,[7] and the effect of surface treatment in the Au/GaAs system.[8] O'Shea *et al.* applied the technique to measure band offset in $Al_xGa_{1-x}As$ with x taking on values of 0.20 and 0.42.[9] Kaiser *et al.* demonstrated that BEEM spectroscopy can be used to extract the L point in the conduction band of AlAs,[10] which lies at an off angle from the growth direction.

In this article, BEEM spectroscopy is used to study the band structure of $Al_xGa_{1-x}As$. The Al compositon x took on many more values so that the material can be examined in both the direct and indirect band gap regime. In additon to

[a]Electronic mail: xcc@ssap.caltech.edu
[b]Present address: Emcore Corp, Somerset, NJ.

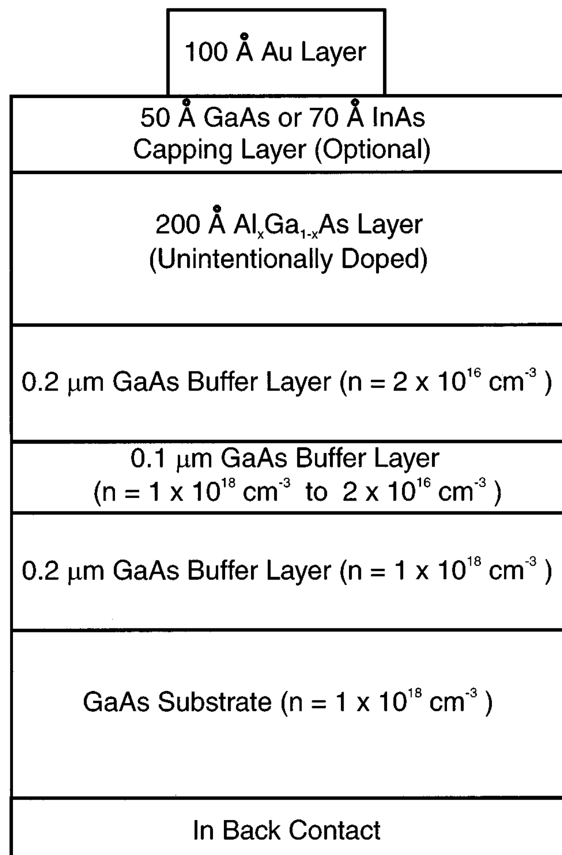

FIG. 1. Structure of a typical BEEM sample.

Schottky barrier height measurements, we have focused on the higher lying conduction band edges in $Al_xGa_{1-x}As$. Unlike the metal on semiconductor Schottky barrier height, the position of the higher lying band edge relative to the bottom of the conduction band is an inherent property of the material. It should not depend on interface chemistry and should also exhibit less local variation. BEEM findings about these band edges can be directly compared to similar results obtained from other techniques. The experiment complements these past studies and helps to clarify any uncertainty about the band edge positions.

II. EXPERIMENT

Samples used in this experiment were grown in a Perkin-Elmer 430 molecular beam epitaxy (MBE) system and metallized *ex situ* with a sputter deposition tool. Figure 1 shows the structure of a typical BEEM sample. We used highly doped ($n=1\times10^{18}$ cm^{-3}) epi-ready GaAs (100) wafers as substrates to ensure that samples would be conductive enough in subsequent BEEM experiments. Following oxide desorption under As over pressure, a buffer layer with a tapered doping profile was grown. The first 0.2 μm of the buffer layer was heavily doped ($n=1\times10^{18}$ cm^{-3}) to match the doping level of the substrate. The doping concentration was gradually decreased to 2×10^{16} cm^{-3} over the next 0.1 μm and maintained at the reduced level over the final 0.2 μm of the buffer layer. At the end of buffer growth, samples were soaked in As for 30 sec, yielding the (2×4) reflection high energy electron diffraction (RHEED) pattern characteristic of reconstructed GaAs surface. An unintentionally doped thin $Al_xGa_{1-x}As$ layer was grown on top of the smoothed GaAs surface. Temperatures of the Al and Ga cells were varied in each growth to give the desired Al concentration in the $Al_xGa_{1-x}As$ layer. The relationship between temperature, growth rate, and Al content had been determined from previous RHEED oscillation studies. The $Al_xGa_{1-x}As$ layer was 200 Å thick for samples with low Al content ($x<0.5$) and 100 Å thick for samples with high Al content. These thicknesses were selected so that bulk properties of $Al_xGa_{1-x}As$ were examined while at the same time the undoped layer was thin enough to support transport of BEEM current. At $x=0.25$, samples with thicknesses of 100 and 200 Å were also grown so that effect due to variation in epilayer thickness could be singled out. Samples with high Al content were capped off at the end of the growth by either a 50 Å GaAs layer or a 70 Å InAs layer to prevent oxidation of the $Al_xGa_{1-x}As$ layer. Samples with low Al content were left uncapped, and a 20–30 Å native oxide layer was present following exposure to the ambient. All GaAs and $Al_xGa_{1-x}As$ layers were grown at a substrate temperature of 570 °C, which was slightly above the GaAs oxide desorption temperature. The InAs capping layer was grown at a reduced substrate temperature of 470 °C.

A sputter-etch deposition system was used for post growth metallization. Gold was sputtered off a solid target by Ar plasma and deposited onto the sample at a rate of 0.7 Å/sec. Samples were placed behind a mask and patterned with arrays of Au dots 1 mm^2 in diameter. Gold layer thickness was monitored by a crystal oscillator and maintained at 100 Å for all samples. Atomic force microscopy (AFM) studies showed that the typical metal layer had a rms roughness on the order of 5 Å. For most samples, the surface morphology was smooth and appeared suitable for BEEM studies. The sputter deposition rate was varied for early samples and was found to have little effect on BEEM results, indicating that sputter damage was not a significant factor.

Prior to metallization, samples were taken out of the ultrahigh (UHV) growth environment and exposed to the ambient. Hence a 20–30-Å-thick native oxide was present between the metal and semiconductor layer. However, Talin *et al.* have shown that the oxide layer does not affect BEEM results for Au/GaAs structures.[11] In fact, samples with native oxide layers support BEEM current more consistently over a longer period of time. In our study, it was found that samples with native oxide layers were stable for up to several months. To minimize contamination from handling, a degreasing procedure was followed before the sample was introduced to the metallization chamber. It consisted of sequential ultrasonic rinse in trichloromethane, acetone, isopropanol and deionized water, with each rinse lasting 2 min. The procedure helped generate more consistent BEEM results, especially for samples that have been stored in air for a long time.

Our BEEM set-up was configured for experiments in air

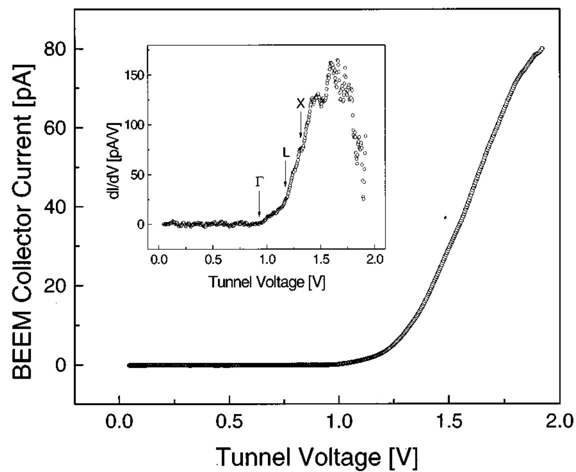

FIG. 2. BEEM I-V curve for $Al_{0.11}Ga_{0.89}As$. Tunnelling current is held constant at 5 nA. The spectrum is averaged over 50 voltage ramps. The inset shows the corresponding differentiated curve. The dI/dV data are fitted to a piecewise linear curve (not shown). Arrows point to the extracted BEEM thresholds, which are attributed to the Γ, L and X points.

at room temperature. It was based on a Digital Instruments scanning tunnelling microscope unit (Nanoscope III). The original microscope head was modified to ground the connections differently. The STM preamplifier had to be rebuilt so that the sample instead of the tip was grounded. The stock sample mount was also replaced by a custom made unit. In the new configuration, a fine Au wire was spring mounted against the top of the sample as the STM base contact. The sample was proxied to a copper plate via conductive silver paint. Indium left from growth, on the backside of the sample, served as the BEEM back contact. BEEM current was first converted to voltage by a Keithley 427 picoammeter before being fed to the stock digital signal processing unit. Digital Instrument software was used to analyze the data and maintain control of the STM head. Prior to the $Al_xGa_{1-x}As$ experiment, the set-up was tested and calibrated with the Au/Si(100) system. We obtained a value of 0.77 eV for the Au on Si Schottky barrier height, in agreement with findings from similar BEEM studies.[6,12]

III. RESULTS AND DISCUSSION

Figure 2 shows a typical BEEM I-V curve from an $Al_xGa_{1-x}As$ sample. The data were averaged over 50 voltage ramps to improve the signal to noise ratio. Since the experiment was carried out in air at room temperature, there was some tip drift even after the system had been given hours to equilibrate. Typically, the tip drifted 5–10 nm during the 10 min it took to complete the 50 ramps. Thus in our case, the spatial resolution of BEEM spectroscopy was drift limited and about an order of magnitude higher than the theoretical limit. The resulting BEEM I-V curve should be considered an average over the same area.

The Bell-Kaiser model was applied to analyze the BEEM I-V curve. In this model, it is assumed that the BEEM I-V curve takes on the form

$$I_c=\sum_{i=1}^{n}(V-V_i)^2,$$

where I_c is the BEEM collector current, V the tunnel voltage and V_i the threshold voltage. There is some controversy about certain assumptions in the derivation of the original model, most notably the lack of scattering and transverse momentum conservation at the metal semiconductor interface. However, an alternative derivation also exists[13] and the equation has been successfully applied to cases where scattering is significant. For example, in Au/Si(111), it was found that band edges which can only be probed with scattering also contribute to the sum.[14] We adapt the Bell-Kaiser model here for simplicity.

Note that each term in the sum only comes in when the tunnel voltage is above the corresponding threshold. As shown in the inset of Fig. 2, differentiating the BEEM I-V curve generates a piecewise linear curve that clearly reveals the multi-threshold nature of the turn on. The I-V curve shown in Fig. 2 was obtained from an $Al_{0.11}Ga_{0.89}As$ sample. Three thresholds were extracted, corresponding to the Γ, L and X points in the $Al_{0.11}Ga_{0.89}As$ layer. Other samples with low Al concentrations ($x=0$, 0.11,0.19,0.25) produced similar BEEM I-V curves. However, the third threshold, attributed to the X point, was not always evident in every run. This may be due to the comparatively large effective mass of the X valley, which tends to weaken the corresponding BEEM turn on. Samples with high Al concentrations ($x=0.50,0.80,1$) also produced BEEM I-V curves that had robust two threshold fits. The thresholds, however, were attributed to the X and L points. For all samples, it was found that the parabolic turn on model breaks down at about 0.5 V above the first threshold, which was expected due to increased scattering of energetic carriers in the metal layer.[15]

The $Al_xGa_{1-x}As$ layer thickness was varied for $x=0.25$. As shown in Fig. 3, thickness variation beyond 100 Å does not significantly affect the measured BEEM thresholds. Thus the measured band edges may be considered bulk properties of $Al_xGa_{1-x}As$. This result agrees with findings from the Au/AlAs study by Kaiser *et al.*, who showed that most of the thickness induced threshold shift occurs over the first few monolayers of the semiconductor.[10]

The effect of a capping layer is shown in Fig. 4. It can be seen that for both Al concentrations, the capping layer has only a slight effect on the BEEM thresholds. In particular, InAs capping layers did not lower the apparent Schottky barrier heights by significant amounts as suggested by Ke *et al.*[16] This may be due to differences in sample growth. Our growth procedures may have resulted in a large number of dangling bonds at the capping layer/$Al_xGa_{1-x}As$ interface, pinning the Fermi level to the middle of the indirect band gap. The capping layer did, however, help to prevent deterioration of the $Al_xGa_{1-x}As$ layer. The uncapped sample in Fig. 4 supported BEEM current for only a few days whereas the capped samples were stable for up to several months.

The BEEM turn on thresholds are interpreted as band

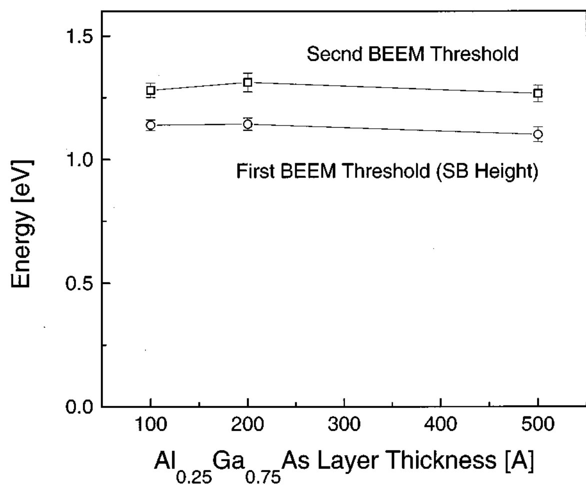

FIG. 3. Variation of BEEM thresholds with $Al_xGa_{1-x}As$ layer thickness. Samples have Al composition $x=0.25$, and were grown and processed under identical conditions.

edges in the semiconductor. The variation of these band edges with Al concentration x is shown in Fig. 5. The extent to which the parabolic model remains valid is also plotted in Fig. 5. Each data point represents 20–30 runs. Since results for $Al_{0.50}Ga_{0.50}As$ indicate that the capping layer does not significantly affect BEEM thresholds, we may view the energy position curves as continua. It can be seen that the Au Schottky barrier height increases with Al concentration x until the semiconductor changes from direct band gap to indirect band gap. For $x<0.45$, the Schottky barrier heights are comparable with those obtained by O'Shea *et al.*[9] even though our samples at these Al concentrations did not have GaAs capping or p-type δ doping. At higher Al concentrations, the Au Schottky barrier height stays almost constant. In particular, our X and L band edge values for AlAs are consistent withfindings by Kaiser *et al.*[10]

To more easily compare the Schottky barrier result with previous findings, it is helpful to plot the implied p-type Schottky barrier height. The p-type Schottky barrier height is obtained by subtracting the n-type Schottky barrier height from the semiconductor band gap. Plotted on the same graph as the band gap as in Fig. 6, it reveals the position of the surface Fermi level in the gap. Our results indicate that the surface Fermi level stays nearly constant at about 0.6 eV from the top of the valence band for $x<0.4$, in accordance with the common anion rule[19] and results obtained by Best.[18] As the material changes from direct band gap to indirect band gap, the surface Fermi level moves towards and stays close to the middle of the indirect band gap.

In general, Schottky barrier height depends on surface treatment and other details of sample preparation. For example, BEEM workers have obtained Au on GaAs Schottky barrier heights that range from 0.82 eV to 0.90 eV.[6,20] The position of the higher lying band edge relative to the first band edge, however, is an intrinsic property of the semiconductor and should be independent of processing. Figure 7 shows the variation of this band edge difference with Al composition x. The plot is derived from BEEM threshold data in Fig. 5 by subtracting the first threshold from the second threshold. The subtraction and error analysis is done for each individual run. Note that the error bars in Fig. 7 are smaller than the sum of threshold error bars in Fig. 5, which shows that the band edge difference is an intrinsic property of the material and has less variation from sample to sample.

In the past, $Al_xGa_{1-x}As$ band edges have been probed by a number of other techniques.[1–4] However, the results from these studies are not totally consistent with each other. Our results agree best with the conductivity findings by Lee *et al.*, which are plotted in Fig. 7 for reference. For $x<0.45$, where $Al_xGa_{1-x}As$ is a direct band gap material, it can be seen that the BEEM threshold difference tracks well with the difference between the L and Γ points as obtained

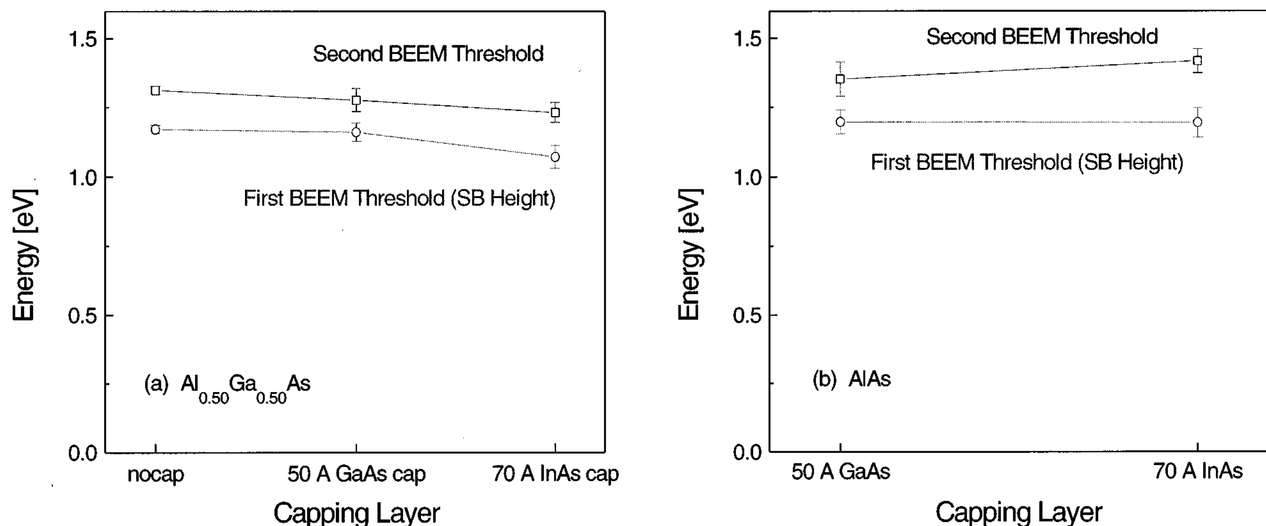

FIG. 4. Effect of capping layer on BEEM thresholds. Samples have Al composition (a) $x=0.50$, and (b) $x=1.0$. Samples in each series are identical except for the capping layer at the end of growth. The GaAs capping layer is 50 Å thick and the InAs capping layer is 70 Å thick.

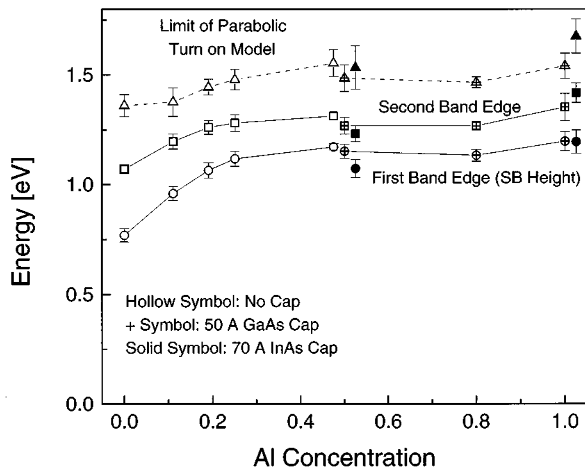

FIG. 5. Variation of $Al_xGa_{1-x}As$ band edges with Al composition x. The dashed curve shows the extent to which the parabolic turn on model remains valid. Samples with low Al content ($x<0.45$) are left uncapped and are represented by hollow symbols. Samples with high Al content ($x>0.45$) are capped with either a 50 Å GaAs layer (+ symbols) or a 70 Å InAs layer (solid symbols). Multiple data points at $x=0.50$ and $x=1.0$ are slightly offset for clarity. Each data point is the result of 20–30 local measurements. The size of the error bars is indicative of local band edge variations.

by Lee *et al.* For $x>0.45$, where $Al_xGa_{1-x}As$ is an indirect band gap material, there is more scatter in the data but BEEM threshold difference agrees well with the difference between the L and X points. Since the L point lies at an off angle from the (100) normal growth direction, its presence in BEEM threshold analysis indicates that there is significant scattering at the metal semiconductor interface. The range over which the parabolic model remains valid is also plotted on the same figure. It can be seen that the Γ point is out of range at high Al concentrations but the X point should have been observed as the third BEEM threshold at low Al concentrations. In fact, the X point turn on was present in some runs. However, it was a weak turn on due to the large effective mass of the X valley, and the results were not consistent enough for systematic analysis.

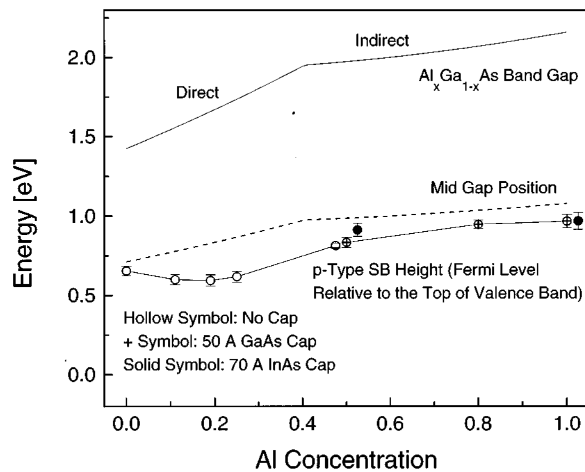

FIG. 6. p-type Schottky barrier height inferred from BEEM data. The data points may also be viewed as the surface Fermi level relative to the top of the valence band. Samples with different capping layers are represented with different symbols. Multiple data points at $x=0.50$ and $x=1.0$ are slightly offset for clarity.

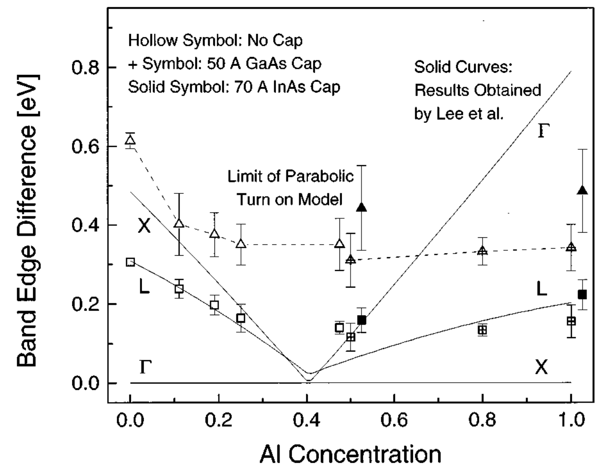

FIG. 7. Difference between the first and second band edges as measured by BEEM. The dashed curve shows the limit of the parabolic turn on model. Results obtained by Lee *et al.* are plotted as solid curves for reference. Samples with different capping layers are represented with different symbols. Multiple data points at $x=0.50$ and $x=1.0$ are slightly offset for clarity.

The spatial variation of the band edges are represented by error bars on the data points. Each error bar is the result of 20 to 30 local measurements. The size of the error bar ranges from 30 to 50 meV, which is comparable with the local variation of Au/GaAs Schottky barrier height obtained by Williams *et al.*[21] Tip drift limited our spectroscopy resolution to about 5–10 nm, which is an order of magnitude higher than the theoretical limit. This may have resulted in less measured variation since BEEM spectroscopy was averaged over a larger area.

IV. SUMMARY

BEEM has been successfully applied to map out band edge shifts in $Al_xGa_{1-x}As$ as the Al concentration x was varied. The study complements past investigations of $Al_xGa_{1-x}As$ band structure, which involved other techniques. Despite the presence of scattering at the metal semiconductor interface, the parabolic turn on model proved to be adequate in the analysis of BEEM spectroscopy data. For $Al_xGa_{1-x}As$ samples in the direct band gap regime ($x<0.45$), the first two BEEM turn on's were attributed to the Γ and L point. For $Al_xGa_{1-x}As$ samples in the indirect band gap regime ($x>0.45$), the turn on's were attributed to the X and L point. The relative positions of these energy points were compared to and found to agree with results from previous studies. The first BEEM turn on also corresponded to the Au on $Al_xGa_{1-x}As$ Schottky barrier height, from which the $Al_xGa_{1-x}As$ surface Fermi level was extracted. The effect of semiconductor layer thickness was examined to ensure that bulk properties were investigated. Various capping layers were also tried and found to have little effect on the measured Schottky barrier height, suggest-

ing Fermi level pinning at the $Al_xGa_{1-x}As$ epilayer surface. This study demonstrates that BEEM spectroscopy is an effective technique for investigating semiconductor band structures.

ACKNOWLEDGMENTS

This study was supported in part by the Office of Naval Research under Grant No. N00019-89-J-00014 and Air Force Office of Scientific Research under Grant No. F49620-93-J-0258. In addition, the authors would like to thank Rob Miles for his part in constructing the BEEM apparatus.

[1] H. C. Casey and M. B. Panish, J. Appl. Phys. **40** 4910 (1969).
[2] B. Monemar, K. K. Shih, and G. D. Pettit, J. Appl. Phys. **47**, 2604 (1976).
[3] A. K. Saxena, Phys. Status Solidi B **105**, 777 (1981).
[4] H. J. Lee, L. Y. Juravel, J. C. Woolley, and A. J. SpringThorpe, Phys. Rev. B **21**, 659 (1980).
[5] W. J. Kaiser and L. D. Bell, Phys. Rev. Lett. **60**, 1406 (1988).
[6] L. D. Bell and W. J. Kaiser, Phys. Rev. Lett. **61**, 2368 (1988).
[7] T.-H. Shen, M. Elliott, A. E. Fowelll, A. Cafolla, B. E. Richardson, D. Westwood, and R. H. Williams, J. Vac. Sci. Technol. B **9**, 2219 (1991).
[8] M. H. Hecht, L. D. Bell, K. W. Kaiser, and F. J. Grunthaner, Appl. Phys. Lett. **55**, 780 (1989).
[9] J. J. OShea, T. Sajoto, S. Bhargava, D. Leonard, M. A. Chin, and V. Narayanamurti, J. Vac. Sci. Technol. B **12**, 2625 (1994).
[10] W. J. Kaiser, M. H. Hecht, L. D. Bell, F. J. Grunthaner, J. K. Liu, and L. C. Davis, Phys. Rev. B **48**, 18 (1993).
[11] A. A. Talin, D. A. Ohlberg, R. S. Williams, P. Sullivan, I. Koutselas, B. Williams, and K. L. Kavanagh, Appl. Phys. Lett. **62**, 2965 (1993).
[12] E. Y. Lee and L. J. Schowalter, Phys. Rev. B **45**, 6325 (1992).
[13] R. Ludeke, Phys. Rev. Lett. **70**, 214 (1993).
[14] M. T. Cuberes, A. Bauer, H. J. Wen, D. Vandre, M. Pretsch, and G. Kaindl, J. Vac. Sci. Technol. B **12**, 2422 (1994).
[15] C. R. Crowell and S. M. Sze, in *Physics of Thin Films*, edited by G. Hass and R. F. Thun (Academic, New York, 1967), p. 325.
[16] M. Ke, D. I. Westwood, C. C. Matthai, and B. Richardson, Mater. Sci. Eng. B **35**, 349 (1995).
[17] Yu. A. Goldberg, T. Yu. Rafiev, B. V. Tsarenkov, and Yu. P. Yakovlev, Sov. Phys. Semicond. **6**, 398 (1972).
[18] J. S. Best, Appl. Phys. Lett. **34**, 522 (1979).
[19] J. O. McCaldin, T. C. McGill, and C. A. Mead, J. Vac. Sci. Technol. **13**, 802 (1976).
[20] A. E. Fowell, R. H. Williams, B. E. Richardson, A. Cafolla, D. I. Westwood, and D. A. Woolf, J. Vac. Sci. Technol. B **9**, 581 (1991).
[21] A. A. Talin, R. S. Williams, B. A. Morgan, K. M. Ring, and K. L. Kavanagh, Phys. Rev. B **49**, 16 (1994).